Notes

Computational Study of Titanocene-Catalyzed Dehydrocoupling of the Adduct $Me_2NH{\cdot}BH_3$: An Intramolecular, Stepwise Mechanism

Yi Luo* and Koichi Ohno*

Department of Chemistry, Graduate School of Science, Tohoku University, Aoba-ku, Sendai 980-8578, Japan

Received April 22, 2007

Summary: The titanocene-catalyzed dehydrocoupling of the adduct $Me_2NH{\cdot}BH_3$ has been investigated by density functional theory (B3LYP). Unlike the thermal dehydrogenation of ammonia−borane, which was previously found to occur via a concerted mechanism, such a catalytic dehydrogenation of $Me_2NH{\cdot}BH_3$ has been found to be a stepwise process. Both intra- and intermolecular dehydrogenation pathways have been computed. The entire intramolecular dehydrogenation process is exergonic by 7.4 kcal/mol, and the intermolecular dehydrogenation is an endergonic process. The solvation free-energy barriers for the intramolecular dehydrogenations are 14.1 and 7.9 kcal/mol, respectively, which are lower than those of the intermolecular dehydrogenation pathway (24.1 and 9.2 kcal/mol, respectively). These results suggest that the intramolecular pathway is preferable both kinetically and energetically. The resulting monomeric aminoborane species, $Me_2N{=}BH_2$, may undergo dimerization leading to the cyclic $(Me_2N{-}BH_2)_2$, which was experimentally observed.

Introduction

Mechanism is an essential aspect of chemistry in general and of catalytic processes in particular. The transition-metal-catalyzed dehydrocoupling of amine−boranes has attracted considerable attention[1] because of not only its application in organic synthesis and importance in the development of hydrogen storage materials[1c,2] but also its advantage of mild temperature.[3] In this context, many experimental studies have been undertaken to explore the mechanistic aspects and the hetero- vs homogeneous mechanism has been well characterized for such kinds of reactions.[1c,4,5] For example, a recent report[4d] demonstrated that a Ti(II) catalyst, $[Cp_2Ti]$, which is generated in situ by the combination of $[Cp_2TiCl_2]$ and 2 equiv of ^{n}BuLi in toluene,[6] homogeneously catalyzes the reaction shown in Scheme 1. Although a concerted mechanism was proposed for the dehydrogenations of ammonia−borane and hydrocarbon−borane,[7,8] it still remains unknown whether the transition-metal-catalyzed hydrogen releases from the amine and borane partners, such as that in the adduct $Me_2NH{\cdot}BH_3$, are stepwise or concerted processes. Moreover, whether the reaction proceeds via an intermolecular or intramolecular mechanism is often arguable for the catalytic dehydrocoupling of the adduct $Me_2NH{\cdot}BH_3$.[1c,5] The computational study reported here suggests that the reaction shown in Scheme 1 follows an intramolecular, stepwise mechanism. Such a stepwise dehydrogenation for amine−boranes, which is proposed for the first time, may shed new light on the mechanism of this process.

Results and Discussion

The intramolecular dehydrocoupling pathway (path I) has been computationally investigated, and the results are shown in Scheme 2, where the schematic representations of optimized

* To whom correspondence should be addressed. Fax: (+) 81-22-795-6580. E-mail: luo@mail.tains.tohoku.ac.jp (Y.L.).

(1) For reviews, see: (a) Gauvin, F.; Harrod, J. F.; Woo, H. G. *Adv. Organomet. Chem.* **1998**, *42*, 363−405. (b) Jaska, C. A.; Bartole-Scott, A.; Manners, I. *Dalton Trans.* **2003**, *21*, 4015−4021. (c) Clark, T. J.; Lee, K.; Manners, I. *Chem. Eur. J.* **2006**, *12*, 8634−8648 and references therein.

(2) (a) Brown, H. C.; Zaidlewicz, M.; Dalvi, P. V. *Organometallics* **1998**, *17*, 4202−4205. (b) Euzenat, L.; Horhant, D.; Ribourdouille, Y.; Duriez, C.; Alcaraz, G.; Vaultier, M. *Chem. Commun.* **2003**, 2280−2281. (c) Jaska, C. A.; Lough, A. J.; Manners, I. *Inorg. Chem.* **2004**, *43*, 1090−1099. (d) Denney, M. C.; Pons, V.; Hebden, T. J.; Heinekey, D. M.; Goldberg, K. I. *J. Am. Chem. Soc.* **2006**, *128*, 12048−12049. (e) Bluhm, M. E.; Bradley, M. G.; Butterick, R., III; Kusari, U.; Sneddon, L. G. *J. Am. Chem. Soc.* **2006**, *128*, 7748−7749. (f) Yoon, C. W.; Sneddon, L. G. *J. Am. Chem. Soc.* **2006**, *128*, 13992−13993. (g) Gutowska, A.; Li, L.; Shin, Y.; Wang, C. M.; Li, X. S.; Linehan, J. C.; Smith, R. S.; Kay, B. D.; Schmid, B.; Shaw, W.; Gutowski, M.; Autrey, T. *Angew. Chem., Int. Ed.* **2005**, *44*, 3578−3582.

(3) (a) Beachley, O. T., Jr. *Inorg. Chem.* **1967**, *6*, 870−874. (b) Ryschkewitsch, G. E.; Wiggins, J. W. *Inorg. Chem.* **1970**, *9*, 314−317. (c) Baumann, J.; Baitalow, F.; Wolf, G. *Thermochim. Acta* **2005**, *430*, 9−14. (d) Benedetto, S. D.; Carewska, M.; Cento, C.; Gislon, P.; Pasquali, M.; Scaccia, S.; Prosini, P. P. *Thermochim. Acta* **2006**, *441*, 184−190.

(4) (a) Braunstein, P.; Morise, X. *Organometallics* **1998**, *17*, 540−550. (b) Jaska, C. A.; Manners, I. *J. Am. Chem. Soc.* **2004**, *126*, 1334−1335, 2698−2699. (c) Jaska, C. A.; Clark, T. J.; Clendenning, S. B.; Grozea, D.; Turak, A.; Lu, Z.-H.; Manners, I. *J. Am. Chem. Soc.* **2005**, *127*, 5116−5124. (d) Clark, T. J.; Russell, C. A.; Manners, I. *J. Am. Chem. Soc.* **2006**, *128*, 9582−9583.

(5) (a) Jaska, C. A.; Temple, K.; Lough, A. J.; Manners, I. *J. Am. Chem. Soc.* **2003**, *125*, 9424−9434. (b) Jaska, C. A.; Manners, I. *J. Am. Chem. Soc.* **2004**, *126*, 9776−9785. (c) Jaska, C. A.; Temple, K.; Lough, A. J.; Manners, I. *Chem. Commun.* **2001**, 962−963. (d) Chen, Y.; Fulton, J. L.; Linehan, J. C.; Autrey, T. *J. Am. Chem. Soc.* **2005**, *127*, 3254−3255.

(6) For the formation and usage of Ti(II) metallocenes, see: (a) Sato, F.; Urabe, H.; Okamoto, S. *Chem. Rev.* **2000**, *100*, 2835−2886. (b) Corey, J. Y.; Zhu, X. H.; Bedard, T. C.; Lange, L. D. *Organometallics* **1991**, *10*, 924−930. (c) Corey, J. Y.; Huhmann, J. L.; Zhu, X. H. *Organometallics* **1993**, *12*, 1121−1130. (d) Hitchcock, P. B.; Kerton, F. M.; Lawless, G. A. *J. Am. Chem. Soc.* **1998**, *120*, 10264−10265. (e) Pender, M. J.; Carroll, P. J.; Sneddon, L. G. *J. Am. Chem. Soc.* **2001**, *123*, 12222−12231.

(7) For uncatalyzed dehydrogenations of ammonia−borane and hydrocarbon−borane, see: (a) Glodfuss, B.; Knochel, P.; Bromm, L. O.; Knapp, K. *Angew. Chem., Int. Ed.* **2000**, *39*, 4136−4139. (b) Li, Q. S.; Zhang, J.; Zhang, S. *Chem. Phys. Lett.* **2005**, *404*, 100−106.

(8) For Lewis acid catalyzed dehydrogenations of ammonia−borane, see: (a) Stephens, F. H.; Baker, R. T.; Matus, M. H.; Grant, D. J.; Dixon, D. A. *Angew. Chem., Int. Ed.* **2007**, *46*, 746−749. (b) Nguyen, M. T.; Nguyen, V. S.; Matus, M. H.; Gopakumar, G.; Dixon, D. A. *J. Phys. Chem. A* **2007**, *111*, 679−690.

10.1021/om7003892 CCC: $37.00
Publication on Web 06/12/2007

Scheme 1. Titanocene-Catalyzed Dehydrocoupling of $Me_2NH{\cdot}BH_3$

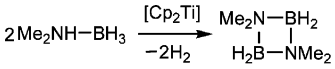

Scheme 2. Intramolecular Dehydrocoupling Pathway (Path I) of the Adduct $Me_2NH{\cdot}BH_3$ Catalyzed by $[Cp_2Ti]$[a]

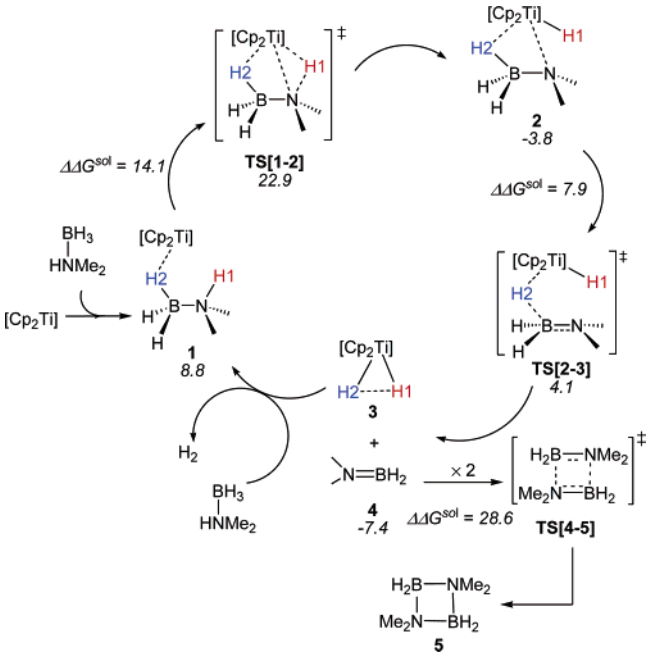

[a] The solvation free energies ($\Delta\Delta G^{sol}$, in kcal/mol) are relative to $[Cp_2Ti]$ and the adduct $Me_2NH{\cdot}BH_3$.

Table 1. Selected Interatomic Distances (in Å) in the Stationary Points Involved in Path I

	1	TS[1-2]	2	TS[2-3]	3	4
N−H1	1.023	1.249	2.371	3.176		
B−H2	1.236	1.277	1.301	1.760		
N−B	1.632	1.621	1.539	1.428		1.391
Ti−H1	3.304	1.820	1.658	1.688	1.677	
Ti−H2	1.986	1.893	1.862	1.711	1.676	
Ti−N	3.742	2.490	2.303	3.442		
Ti−B	3.171	2.590	2.579	3.190		

stationary points and the relative solvation free energies are given. In path I, the dehydrocoupling starts with the coordination of one $Me_2NH{\cdot}BH_3$ adduct to the Ti center via a hydrogen atom of the BH_3 moiety (**1** in Scheme 2)[9] and then proceeds through a transition state (TS), **TS[1-2]**, leading to **2** with a newly formed Ti−H1 bond and Ti···N interaction, as suggested by Ti−H1 (1.66 Å) and Ti···N contacts (2.30 Å), respectively (Table 1). It is noteworthy that the **TS[1-2]** has a five-membered cyclic structure constructed by Ti, H1, N, B, and H2 atoms, in which the interaction between the Ti and the N (B) atom is involved.[10]

(9) The coordination via amine partner made the complex less stable by ~5 kcal/mol compared to **1**. From the point of view of the thermodynamics, we could not further investigate the reaction of such a less stable coordination complex. Although a complex coordinated in an η^3 fashion via the B atom and two hydrogens of BH_3 (see **1c** in Figure S-3, Supporting Information) was computed to be more stable by 3.5 kcal/mol in comparison with **1**, its dehydrogenated product via cleavage of a (μ_2-H)−B bond was not computationally obtained (see Figure S-4, Supporting Information), probably because it is hard for the μ_2-H in the η^3-coordinated complex to adopt the μ_1 mode to bond to the Ti atom, when the partially dehydrogenated species $H_2B{-}NHMe_2$ has no additional binding partner.

(10) Such a cyclic structure and the Ti···N and Ti···B interactions in **TS[1-2]** are suggested by the corresponding interatomic distances (see Table 1). These features of **TS[1-2]** can be also seen from the molecular orbital isosurface (see Figure S-11, Supporting Information).

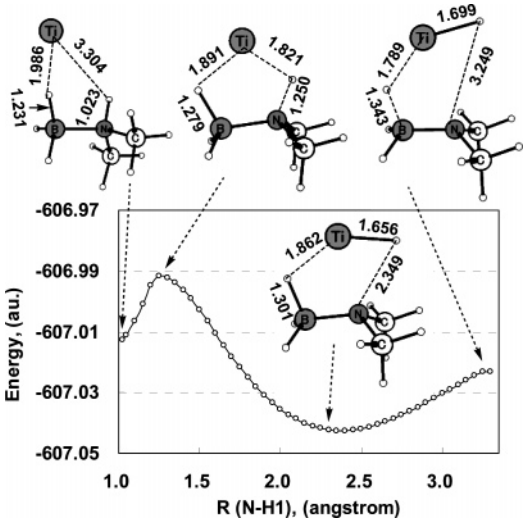

Figure 1. Computed PES for the dehydrogenation along path I. In the structures, the Cp ligands are omitted for clarity and the unlabeled balls denote hydrogen atoms. The distances are given in Å.

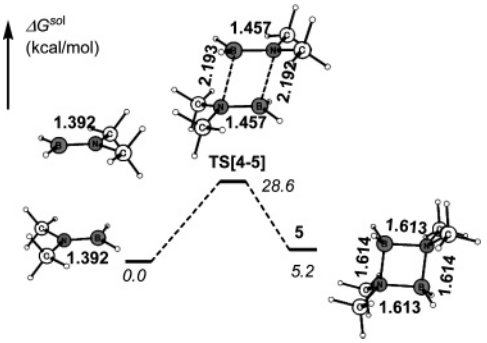

Figure 2. Dimerization of **4**. Unlabeled balls denote hydrogen atoms, and the double bonds are not shown here. The distances are given in Å.

The conversion of **1** to **2** needs to overcome a solvation free energy barrier of 14.1 kcal/mol. This dehydrogenation (cleavage of the N−H1 bond) process is exergonic by 3.8 kcal/mol relative to separate $[Cp_2Ti]$ and $Me_2NH{\cdot}BH_3$. The intermediate **2** proceeds to undergo further dehydrogenation by passing **TS-[2-3]** with an energy barrier of 7.9 kcal/mol, giving the aminoborane $H_2B{=}NMe_2$ (**4**) and the complex Cp_2TiH_2 (**3**), as can be seen from the B−N bond length (1.39 Å) in **4** and the Ti−H1 and −H2 bond lengths (1.68 Å) (see Table 1) in **3**.

The whole dehydrogenation process in path I is exergonic by 7.4 kcal/mol. The **3** could easily release H_2, possibly by access of an incoming $Me_2NH{\cdot}BH_3$ adduct. However, the unsaturated species **4,** which was previously observed as an intermediate,[4d] may undergo dimerization leading to cyclic **5** via **TS[4-5]**, as shown in Figure 2. There is a solvation free energy barrier of 28.6 kcal/mol for the conversion of **4** to **5**, during which the formations of two B−N bonds are concerted. The dehydrogenations along with path I occur via two individual TSs, viz. **TS[1-2]** and **TS[2-3]**, which are separated by the partially dehydrogenated intermediate **2** along the minimum-energy pathway, suggesting a stepwise dehydrogenation process.

To further determine whether the dehydrogenations along path I are stepwise, the relaxed potential energy surface (PES) against the N−H1 distance was scanned at the same level of theory. The result, which is shown in Figure 1, indicates the regions around **TS[1-2]** (with an N···H1 contact of 1.25 Å) and **2** (with an N···H1 contact of 2.35 Å), respectively, suggesting a stepwise

Scheme 3. Intermolecular Dehydrocoupling Pathway (Path II) of the $Me_2NH{\cdot}BH_3$ Adduct Catalyzed by $[Cp_2Ti]$[a]

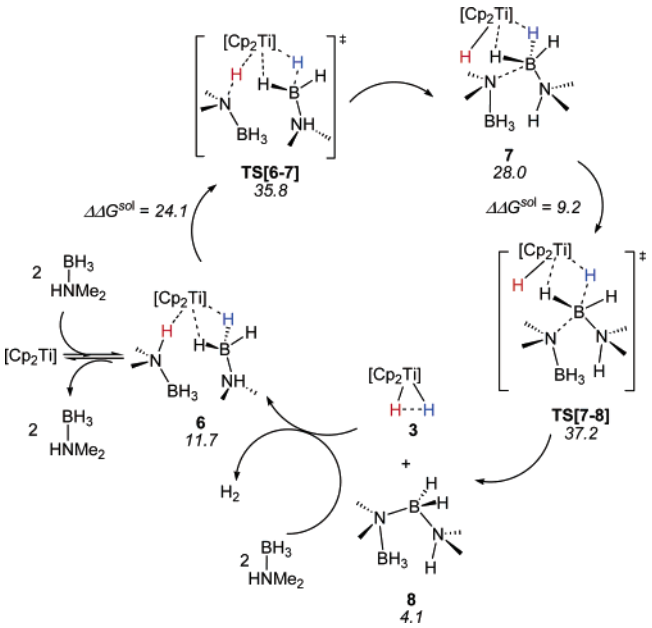

[a] The solvation free energies ($\Delta\Delta G^{sol}$, in kcal/mol) are relative to $[Cp_2Ti]$ and the substrates.

dehydrogenation process. Actually, all attempts to find a concerted dehydrogenation pathway were fruitless.

In view of the energy barriers for the two-step dehydrogenations, the conversion of **1** to **2** is the rate-determining step in the hydrogen release process. Hence, the factors stabilizing the structure of **TS[1-2]**, such as that strengthening the Ti···N or Ti···B interactions in **TS[1-2]**,[10] may accelerate H_2 release. The energy barrier for the dimerization of **4** (28.6 kcal/mol) (see Figure 2) is significantly higher than that for the conversion of **1** to **2** (14.1 kcal/mol), suggesting that the formation of dimer **5** is slower than the hydrogen release. This result may explain the fact that species **4** was experimentally observed at the initial stage and that byproducts appeared during the reaction.[4d,11]

The finding that a heterogeneous Rh metal catalyst induced an intermolecular hydrogen release from amine−borane adducts[5a] caused us to wonder whether the current catalyst behaves similarly. For this purpose, we also computed the intermolecular dehydrogenation pathway (path II), which is shown in Scheme 3. The intermolecular dehydrogenation process starts with the formation of complex **6** with the coordination of two $Me_2NH{\cdot}BH_3$ adducts,[12] in which one of the two $Me_2NH{\cdot}BH_3$ adducts coordinates in a η^3 fashion to the Ti center via B and two hydrogens of the BH_3 moiety and the other adduct coordinates through the amine hydrogen of the $HNMe_2$ partner. Then, **6** undergoes cleavage of a N−H bond by passing **TS[6-7]**, leading to complex **7** having a partially dehydrogenated $Me_2N{-}BH_3$ species, which weakly interacts with the other amine−borane adduct. The intermediate **7** further undergoes dehydrogenation via **TS[7-8]** with a barrier of 9.2 kcal/mol, leading to the complex **3** and species **8**. It was previously reported that **8** took 2 days to convert to **5** in the presence of Rh metal catalyst.[5a] We could not further investigate the catalytic conversion of **8** to **5** in the current system, since path II is an unfavorable reaction pathway (vide infra). However, the observed conversion of **8** to **5** stimulated our interest in the H_2 release from **8**. We computationally investigated the uncatalyzed H_2 release process of **8** by using the sphere contracting walk (SCW) and two-point scaled hypersphere search (SHS) methods.[13] It was found that the H_2 release from **8** was preferably concerted with the formation of 2 equiv of **4** (a precursor of **5**) rather than ring closure directly leading to **5**. The gas-phase free energy barrier for such a transformation was computed to be 29.9 kcal/mol, which is slightly lower than that for the H_2 elimination of $H_3N{\cdot}BH_3$ under thermal condition (32∼37 kcal/mol)[7,8b] (see Figure S-6 in the Supporting Information for more details). An analysis of the imaginary mode of **TS[7-8]** shows that the intermolecular coupling via the formation of a new B−N bond is concerted with the cleavage of a B−H bond (see Figure S-5 in the Supporting Information). The acyclic species **8** has the newly formed $(Me_2NH)H_2B{-}NMe_2(BH_3)$ bond.

However, at the primary dehydrogenation step, the conversion of **6** to **7** (solvation free energy barrier of 24.1 kcal/mol and endergonic by 28.0 kcal/mol) in path II is neither energetically nor kinetically favored in comparison with the conversion of **1** to **2** (energy barrier of 14.1 kcal/mol that is exergonic by 3.8 kcal/mol) in path I. Moreover, the relative solvation free energy of **TS[6-7]** (35.8 kcal/mol) (see Scheme 3) is significantly larger than that of **TS[1-2]** (22.9 kcal/mol) (see Scheme 2). These results suggest that the dehydrocoupling process preferably follows an intramolecular pathway (path I).[14]

In summary, the titanocene-catalyzed dehydrocoupling of the adduct $Me_2NH{\cdot}BH_3$ has been computationally found to proceed through intramolecular, stepwise dehydrogenation followed by dimerization of the resulting monomeric aminoborane species.

Computational Details

The geometry optimizations and energy estimations were carried out by the method of hybrid B3LYP density functional theory.[15] The 6-31G* basis set was considered for the C and H atoms of Cp ligands and the Me groups of $Me_2NH{-}BH_3$. The B, N, and remaining hydrogen atoms, which are related to the formation/dissociation of chemical bonds, were treated by the 6-31++G** basis set. The LanL2DZ effective core potentials and the associated basis set[16] were used for the Ti atom. The toluene solvation and gas-phase optimizations (with and without an augmentation of f-polarization function[17] for Ti) of the $[Cp_2Ti]$ structure show very little variations in geometry (Figure S-1 in the Supporting Information), suggesting that f-function and toluene solvation effect do not

(11) During the reaction, the signal of a byproduct appeared and was tentatively assigned to the cyclic trimer $[Me_2N{-}BH_2]_3$.[4d] As suggested in the same work, the cyclic trimer possibly resulted from the trimerization of **4**, which should be less favorable than dimerization. We have also computationally found that the dissociation of this cyclic trimer leading to **5** and **4** is exergonic by 12.6 kcal/mol in solution, suggesting that the trimer can easily convert to the dimer **5**. A small signal was also observed in the NMR spectrum during the reaction, which was assigned to the byproduct $Me_2N{-}BH{-}NMe_2$.[4d] Since the transformation shown in Scheme 1 is fully achieved, the reaction route leading to the $Me_2N{-}BH{-}NMe_2$ species is not preferred over path I (Scheme 2) and hence was not investigated in this study.

(12) For complex **6**, attempts to computationally model a possible dehydrogenation product with the breakage of a (μ_2-H)−B bond were unsuccessful, leading to complex **6** instead. This situation is similar to the case of **1c**.[9]

(13) Maeda, S.; Ohno, K. *J. Chem. Phys.* **2006**, *124*, 174306; *Chem. Phys. Lett.* **2005**, *404*, 95−99.

(14) The preference of the conversion of **1** to **2** over that of **6** to **7** is also suggested by the IRC following curves of **TS[1-2]** and **TS[6-7]** (see Figure S-7 and Figure S-9, Supporting Information).

(15) (a) Beck, A. D. *J. Chem. Phys.* **1993**, *98*, 5648−5652. (b) Lee, C. T.; Yang, W. T.; Parr, R. G. *Phys. Rev. B* **1988**, *37*, 785−789.

(16) (a) Hay, P. J.; Wadt, W. R. *J. Chem. Phys.* **1985**, *82*, 270−283. (b) Wadt, W. R.; Hay, P. J. *J. Chem. Phys.* **1985**, *82*, 284−298. (c) Hay, P. J.; Wadt, W. R. *J. Chem. Phys.* **1985**, *82*, 299−310.

(17) Ehlers, A. W.; Böhme, M.; Dapprich, S.; Gobbi, A.; Höllwarth, A.; Jonas, V.; Köhler, K. F.; Stegmann, R.; Veldkamp, A.; Frenking, G. *Chem. Phys. Lett.* **1993**, *208*, 111−114.

change significantly the geometry of the complex. Hence, the f-polarization function was not augmented during the computations and toluene solvation energy calculations were carried out on the basis of the gas-phase optimized geometries. The solvation energy calculations were carried out by using the CPCM model,[18] which has been widely used for investigation of the solvation effect in various metal complex systems.[19] To consider the entropy effect, the Gibbs free energy contributions from the gas-phase calculations were added to give the final solvation free energies, ΔG^{sol} (298 K, 1 atm).[20] The computed gas-phase electronic energy, enthalpy, and free energy are provided in the Supporting Information. The difference between enthalpy and free energy reflects the contribution of entropy. To see whether the obtained results depend on the selected density functional, the MPW1K density functional,[21] which was developed by Truhlar's group, was also used in some calculations. It was found that the relative energies computed by MPW1K are very similar to those computed by B3LYP (variation of less than 1.7 kcal/mol; see Table S-1 in the Supporting Information), which suggests that the B3LYP method is reliable for computing the energies of the current system. Normal-coordinate analyses were performed to verify the geometrically optimized stationary points and to obtain thermodynamic data. For transition structures, intrinsic reaction coordinate (IRC) routes in both directions to the corresponding minima were calculated, and further geometrical releases to the minima along with both sides were performed for some TSs. The stabilities of wavefunctions were tested. A C_1-symmetry point group was used throughout all calculations, and no higher molecular symmetry restriction was imposed. All calculations were performed utilizing the Gaussian 03 program.[22]

Acknowledgment. We thank Dr. Satoshi Maeda for his technical assistance. Y.L. acknowledges the Japan Society for the Promotion of Science (JSPS) for support of this research.

Supporting Information Available: Figures and tables giving the optimized 3D structures, Cartesian coordinates, total electronic energies, enthalpies, and free energies (gas phase) of all stationary points involved in paths I and II, IRC following results and the imaginary frequencies of TSs, and others. This material is available free of charge via the Internet at http://pubs.acs.org.

OM7003892

(18) (a) Barone, V.; Cossi, M. *J. Phys. Chem. A* **1998**, *102*, 1995−2001. (b) Cossi, M.; Rega, N.; Scalmani, G.; Barone, V. *J. Comput. Chem.* **2003**, *24*, 669−681.

(19) For examples, see: (a) Vallet, V.; Wahlgren, U.; Grenthe, I. *J. Am. Chem. Soc.* **2003**, *125*, 14941−14950. (b) Clot, E.; Eisenstein, O.; Weng, T.-C.; Penner-Hahn, J.; Caulton, K. G. *J. Am. Chem. Soc.* **2004**, *126*, 9079−9084. (c) Holscher, M.; Keul, H.; Hocker, H. *Macromolecules* **2002**, *35*, 8194−8202. (d) Luo, Y.; Hou, Z. *Organometallics* **2006**, *25*, 6162−6165.

(20) Matxain, J. M.; Ristila, M.; Strid, A.; Eriksson, L. A. *J. Phys. Chem. A* **2006**, *110*, 13068−13072.

(21) (a) Lynch, B. J.; Fast, P. L.; Harris, M.; Truhlar, D. G. *J. Phys. Chem. A* **2000**, *104*, 4811−4815. (b) Lynch, B. J.; Truhlar, D. G. *J. Phys. Chem. A* **2001**, *105*, 2936−2941.

(22) Frisch, M. J.; Trucks, G. W.; Schlegel, H. B.; Scuseria, G. E.; Robb, M. A.; Cheeseman, J. R.; Montgomery, J. A., Jr.; Vreven, T.; Kudin, K. N.; Burant, J. C.; Millam, J. M.; Iyengar, S. S.; Tomasi, J.; Barone, V.; Mennucci, B.; Cossi, M.; Scalmani, G.; Rega, N.; Petersson, G. A.; Nakatsuji, H.; Hada, M.; Ehara, M.; Toyota, K.; Fukuda, R.; Hasegawa, J.; Ishida, M.; Nakajima, T.; Honda, Y.; Kitao, O.; Nakai, H.; Klene, M.; Li, X.; Knox, J. E.; Hratchian, H. P.; Cross, J. B.; Bakken, V.; Adamo, C.; Jaramillo, J.; Gomperts, R.; Stratmann, R. E.; Yazyev, O.; Austin, A. J.; Cammi, R.; Pomelli, C.; Ochterski, J. W.; Ayala, P. Y.; Morokuma, K.; Voth, G. A.; Salvador, P.; Dannenberg, J. J.; Zakrzewski, V. G.; Dapprich, S.; Daniels, A. D.; Strain, M. C.; Farkas, O.; Malick, D. K.; Rabuck, A. D.; Raghavachari, K.; Foresman, J. B.; Ortiz, J. V.; Cui, Q.; Baboul, A. G.; Clifford, S.; Cioslowski, J.; Stefanov, B. B.; Liu, G.; Liashenko, A.; Piskorz, P.; Komaromi, I.; Martin, R. L.; Fox, D. J.; Keith, T.; Al-Laham, M. A.; Peng, C. Y.; Nanayakkara, A.; Challacombe, M.; Gill, P. M. W.; Johnson, B.; Chen, W.; Wong, M. W.; Gonzalez, C.; Pople, J. A. *Gaussian 03*, revision C.02; Gaussian, Inc.: Wallingford, CT, 2004.